Journal of Atmospheric Chemistry **28:** 29–44, 1997.

Regional and Global Tropopause Fold Occurrence and Related Ozone Flux Across the Tropopause

M. BEEKMANN[1], G. ANCELLET[1], S. BLONSKY[4], D. DE MUER[3], A. EBEL[2], H. ELBERN[2], J. HENDRICKS[2], J. KOWOL[2], C. MANCIER[1], R. SLADKOVIC[5], H. G. J. SMIT[6], P. SPETH[4], T. TRICKL[5] and Ph. VAN HAVER[3]

[1]*Service d'Aéronomie du CNRS, Université Paris 6, Boîte 102, 75252 Paris Cedex 05, France*
[2]*University of Cologne, EURAD project, Institute for Geophysics and Meteorology, Aachener Str. 201–209, D-50923 Köln, Germany*
[3]*Meteorological Institute of Belgium (KMI), Ringlaan 3, B-1180 Brussels, Belgium*
[4]*University of Cologne, Institute for Geophysics and Meteorology, Kerpener Str. 13, D-50923 Köln, Germany*
[5]*IFU, Kreuzeckbahnstr. 19, D-82467 Garmisch-Partenkirchen, Germany*
[6]*Forschungszentrum Jülich, ICG-2, P.O. Box 1913, D-52425 Jülich, Germany*

(Received: 15 April 1996; in final form: 17 April 1997)

Abstract. This paper gives a synthesis of three algorithms to detect the presence of tropopause folds from vertical ozone/radio-sounding profiles and from meteorological analysis. Also an algorithm to identify injection of stratospheric air into the lower troposphere from ozone/^{7}beryllium time series is presented. Differences in the results obtained from the algorithms are observed and discussed with respect to the criteria for fold detection and input data used. Spatial gradients in the obtained folding frequencies are made evident on a global scale from the algorithm based on meteorological analysis (Q-vector/potential vorticity) and probably also on a regional European scale from algorithms both based meteorological analyses and on ozone/PTU soundings. The observed seasonal variation of folding occurrence is rather flat except during summer when also some differences appear between the algorithms. By combining the folding frequencies with literature estimates of the cross-tropopause ozone transfer in single folding events, an average stratospheric ozone influx into the troposphere of $5.7 \pm 1.3 \times 10^{10}$ mol. cm^{-2} s^{-1} is obtained for the Northern hemisphere and $12 \pm 2.7 \times 10^{10}$ mol. cm^{-2} s^{-1} for Western Europe. Potential additional contributions due to other stratosphere-troposphere exchange processes than folds are not yet included in these estimates. Finally, the link between statistics from ozone/^{7}beryllium data and folding statistics is briefly discussed.

Key words: stratosphere-troposphere exchange, tropopause folding, cross tropopause, ozone transfer, vertical ozone profiles, potential vorticity, Q-vector divergence, ^{7}beryllium.

1. Introduction

One of the goals of the EUROTRAC/TOR project was to determine the influx of stratospheric ozone into the European free troposphere and to compare it to photochemical ozone production in the free troposphere and upward ozone transport from the atmospheric boundary layer. Recently, Holton *et al.* (1996) argued that stratosphere-troposphere exchange (STE) may best be conceptually under-

stood using the 'downward control principle' and quantified by examining the residual mean circulation at control levels in the lower stratosphere. Nevertheless, detailed knowledge about transport processes acting at the tropopause level (e.g., tropopause folds or cut-off lows) is required to determine the geographical and temporal distribution of STE and the cross-tropopause flux of species with a significant chemical source or sink in the lowermost stratosphere (e.g., NO_x, ozone when heterogeneous chemistry is active). Tracer and in particular ozone transport during tropopause fold events and to some extent also within cut-off lows has been addressed in many works (e.g., Danielsen, 1968; Shapiro, 1980; references given in Table II). While the frequency of cut-off lows has been established in several studies some years ago (e.g., Price and Vaughan, 1992) the occurrence of tropopause folds has been determined in a systematic way only most recently: folds were detected in vertical ozone/PTU/wind profiles as ozone rich, dry, stable layers located in an upper level front (Van Haver *et al.*, 1996) or as ozone rich, dry, PV (potential vorticity) rich layers (Speth *et al.*, 1996) located in the jet stream area. On a global scale, tropopause fold occurrences have been derived from meteorological analyses by seeking for combined maxima of Q-vector divergence and PV in the upper troposphere (Ebel *et al.*, 1996).

The first aim of this paper is to synthesise and intercompare results obtained with the three above mentioned methods to detect tropopause folds. Second, by combining the obtained fold occurrences with literature estimates of ozone transfer in individual folding events the average ozone flux across the tropopause will be derived and compared to previously given values. Transport of stratospheric air into the lower troposphere is important as it may indirectly affect even ozone concentrations at ground and will be assessed in this paper from ozone and ^{7}beryllium time series recorded at mountain stations. This work was performed in the frame of TOR task group 3b aiming at establishing climatologies of ozone transport from the stratosphere into the troposphere on a regional and global scale (Beekmann *et al.*, 1997).

2. Tropopause Fold Detection Algorithms

Tropopause folds typically occur in connection with baroclinic waves and upper-level frontogenesis in the upper tropospheric polar, and to a lesser extent also arctic and subtropical jet stream region (e.g., Danielsen, 1968). Frontogenetically induced ageostrophic circulation forces stratospheric air down into the troposphere resulting in a folding of the dynamical tropopause defined as a constant potential vorticity (PV) surface (e.g., at the 1.6 PVU (1 PVU $= 10^{-6}$ Km^2 kg^{-1} s^{-1}) level). Turbulent and diabatic mixing across the fold edges causes irreversible transfer of stratospheric tracers such as ozone, PV, cosmogenic radionuclids (e.g., ^{7}beryllium), which are all maximum in the fold, and humidity, which is minimum, into the troposphere. Tropopause folds can be detected either by tracking the related dynamical processes or the related tracer transport. All algorithms presented in this

section make use of a combination of several of the fold characteristics outlined above and need different input of either experimental or meteorological assimilation data. In this section only a brief synthesis of the algorithms will be given, more details may be found in the specific references given below and in Beekmann *et al.* (1997).

The algorithm developed by KMI (Ph. Van Haver, D. De Muer) and Service d'Aéronomie/CNRS (M. Beekmann, C. Mancier, and G. Ancellet) (Van Haver *et al.*, 1996) detects tropopause folds as ozone rich, stable and dry layers in an ozone/radio-sounding profile as, for example, shown in Figure 1. The threshold values used in the algorithm are (i) an ozone mixing ratio enhanced by at least 25% compared to the climatological mean and compared to adjacent minima in the ozone profile, (ii) a vertical potential temperature gradient larger than 11.5 K/100 hPa and (iii) relative humidity below 25%. In addition, these layers have to be located (iv) in the vicinity of an upper tropospheric jet stream and (v) within an upper level front. The former condition corresponds to a threshold of 20 m s^{-1} to be exceeded in the wind profile, the latter condition corresponds via the thermal wind equation to a strong vertical wind shear to be observed in the folding region (>5 ms^{-1} km^{-1} over at least 2 km). The correct working of the algorithm was verified for a test period (1991–1992) by analysing weather maps and cross-sections (potential temperature, wind, PV) constructed from ECMWF assimilations. With few exceptions, all cases detected with the automatic algorithm were identified as folds with the control algorithm.

The algorithm developed at the University of Cologne by S. Blonsky and P. Speth (Speth *et al.*, 1996) requires significantly enhanced (>20 ppb) ozone values in the folding region as compared to a climatological background profile from which cases displaying tropopause folds are iteratively removed. Relative humidity has to be low ($<20\%$). In addition, the PV vertical profile (computed from ECMWF analysis) has to display a distinct maximum above 1 PVU within 100 hPa above or below the pressure of the detected enhanced ozone concentrations. PV values above one PVU suggest at least a partly stratospheric origin of an air mass (Shapiro *et al.*, 1980). The prerequisite of a *layer* of enhanced PV values excludes cases of simply lowered dynamical tropopause and ozonopause which may be connected to troughs or cut-off lows without necessarily indicating the presence of a tropopause fold. A last criterium about the wind speed in the tropopause region (>30 m s^{-1}) makes sure the presence of an upper tropospheric jet stream. The latter two conditions were not yet implemented in the version of the algorithm presented in Beekmann *et al.* (1997). For each profile positively identified by this procedure (e.g., as the profile in Figure 1) and also for each sounding performed during one year, the meteorological situation has been inspected. It turned out that only a few of the soundings were wrongly associated with tropopause folds and that the algorithm detects virtually the same set of folds as displayed by full meteorological analysis.

In an algorithm developed by the EURAD group (J. Hendricks, H. Elbern and A. Ebel) (Ebel *et al.*, 1996) tropopause folds are identified with the aid of a pattern

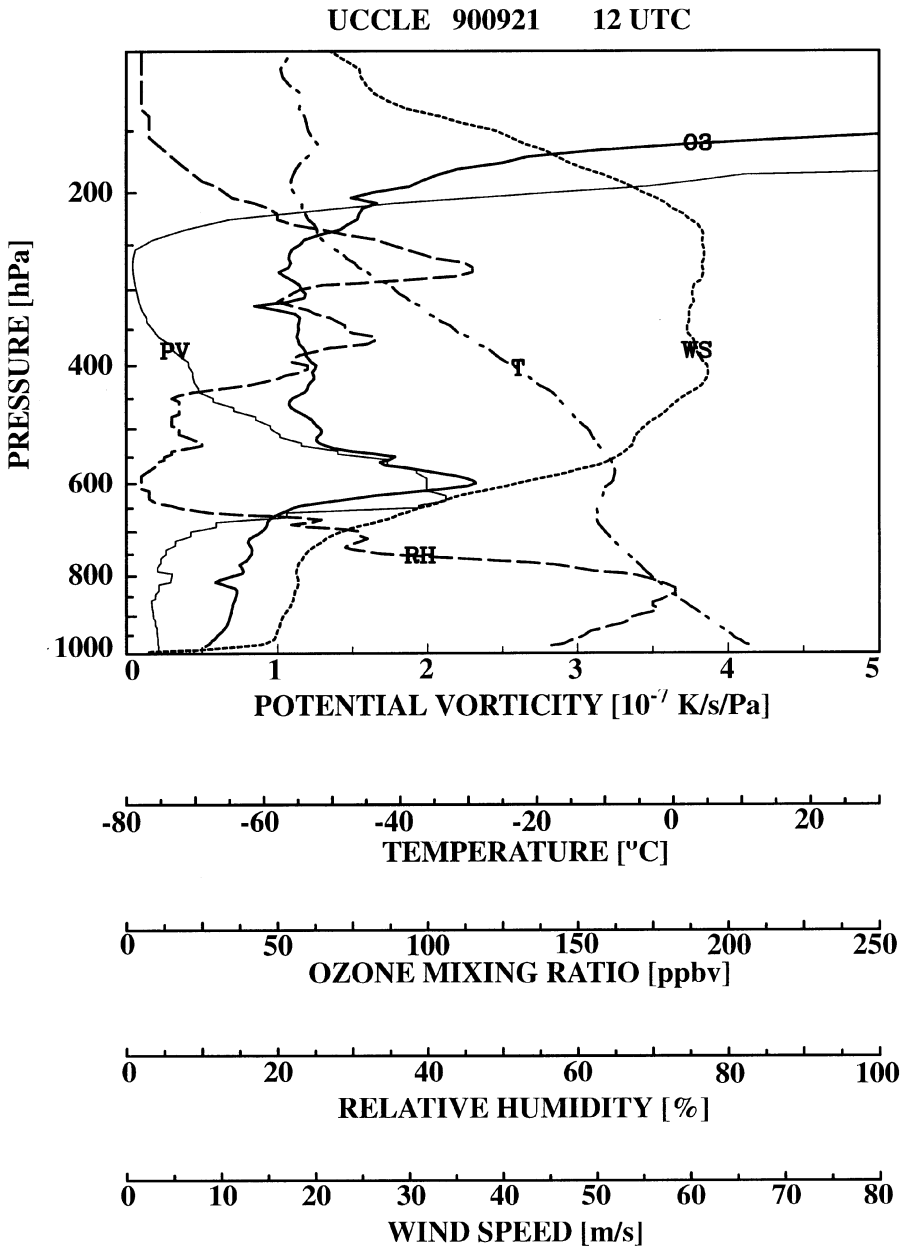

Figure 1. Vertical profiles of ozone mixing ratio (O_3), temperature (T), relative humidity (RH), wind speed (WS) and calculated potential vorticity (PV), for the 21.9.1990 at 12 UTC at Uccle.

matching algorithm which checks the occurrence of upper tropospheric Q-vector divergence maxima ($>1 \times 10^{-15}$ Km^{-2} s^{-1} averaged over the 400 and 500 hPa level) in connection with maxima of potential vorticity (>1.6 PVU at 400 hPa). The

Q-vector divergence maximum corresponds to frontogenetically induced subsiding vertical motion and its strength is used to rate the activity of the folding. Both Q-vector divergence and PV are derived from objective meteorological analyses thus allowing fold statistics to be obtained on a global scale. In order to determine threshold values for both identification criteria in an objective manner, a reference data base of folds in the Atlantic/Europe region was constructed from simulations with the 3D mesoscale EURAD model (*EUR*opean *A*cid *D*eposition model) and the pair of threshold values was chosen which best fitted the reference data base.

Although the formation mechanisms of tropopause folds are now well understood, detailed knowledge to which extent intruded air masses succeed in entering the lower troposphere, the planetary boundary layer, or even the ground level, is still lacking. The objective of a study done by the EURAD group (J. Kowol, H. Elbern and A. Ebel) (Elbern *et al.*, 1996) is to assess frequency and intensity of stratospheric air intrusions into the lower troposphere and to analyse the spatial and temporal distances between a tropopause fold and its signal observed in the lower troposphere. Time series of ozone, ^{7}beryllium and relative humidity measured at two nearby mountain sites (Zugspitze, 2962 m a.s.l. and Wank, 1776 m a.s.l.) in the Northern Alps are analysed over a time span of 10 years. Episodes are idetified as stratospheric intrusions if they show an increase in ^{7}beryllium activity of at least twice the standard deviation of the monthly mean, a significant increase in ozone concentration and decrease in relative humidity (Elbern *et al.*, 1996). Also, the analysis of the synoptical situation has to show that upper level frontogenesis occurs over Western and Central Europe and TOMS data has to display a maximum of the ozone column. Cases of recent photochemical ozone production are evident by analysing the cross-correlation of ozone and NO_2 and the correlation of ozone and SO_2 and are rejected. Detailed numerical studies of selected episodes with the MM5 mesoscale model of the EURAD group and trajectory analyses, based on wind fields calculated with MM5, reveal a direct dynamical link between tropopause folds and ozone^{7}beryllium activity maxima on the Zugspitze summit.

3. Tropopause Fold Occurrences and Ozone Injection into the Lower Troposphere

Table I summarises the European ozone/PTU-sounding data used for tropopause fold detection with the KMI/CNRS and the University of Cologne algorithms and the obtained results. Averaged over several years, folds are detected with the KMI/CNRS algorithm in 3–5% and with the University of Cologne algorithm in 0–2% of the soundings for different stations. At the Uccle station and for the years 1989–1992, when both algorithms could be directly compared, about two and a half times more tropopause folds are detected with the KMI/CNRS algorithm (22 cases) than with the University of Cologne algorithm (9 cases). These differences will be addressed in more detail in the next section.

Table I. Data base of ozone/radio-soundings used for fold detection, number and fraction of detected folds

Station	Uccle	Jülich	Hohenpeissenberg	Payerne
(a) *University of Cologne algorithm*				
Location	51° N4° E	51° N6° E	48° N11° E	47° N7° E
Year	1989–92[a]	1990–92[a]	1989–92[a]	1989–92[a]
Number of folds	9	4	0	2
Number of profiles	554	289	477	526
Fraction folds	2%	1%	0%	0%
Station	Uccle	OHP	Biscarosse	
(b) *KMI/CNRS algorithm*				
Location	51° N4° E	44° N6° E	43° N1° W	
Year	1969–94	1985–94	1976–83	
Number of folds	133	10	10	
Number of profiles	2733	340	335	
Fraction folds	4.8%	3%[b]	3%	

[a] The University of Cologne algorithm was applied for the years 1989–1992 for which potential vorticity derived from ECMWF analyses has been computed.
[b] The fraction of folds detected at OHP has increased from 2% in the study of Van Haver *et al.* (1996) to 3% in this study by taking additionally into account the year 1994.

The identification scheme based on the occurrence of a joint Q-vector divergence and PV maximum, was applied to a data set of 10 years (Dec. 1983–Nov. 1993) of daily ECMWF global analyses with a 2.8° horizontal resolution. Figure 2 shows that, on the average, folds occur twice as much in the Northern than in the Southern Hemisphere. In the Northern Hemisphere they are concentrated in the latitude band 40–70 degrees. Regional maxima occur in the east of North America and Asia and in Europe. On the average, 18.4 folds are simultaneously present in the Northern Hemisphere. Previously, Viezee *et al.* (1983) have assumed that one folding occurs in each of the 4–4.5 major mid-tropospheric low pressure systems simultaneously present in the Northern Hemisphere. The Ebel *et al.* (1996) study shows now that tropopause folds are certainly often detected in the front side of troughs, but also in their rear and in regions of zonal flow of the polar jet stream. Moreover, folds also appear outside of mid-latitudes north of 60°, during northerly excursions of the polar jet stream or in conjunction with the arctic jet stream as described for example for a case study by Shapiro *et al.* (1986).

A climatology of stratospheric intrusions (Elbern *et al.*, 1996) into the lower troposphere was obtained from a 10 year time series (1984–1993) of ozone, ^{7}Be and relative humidity measurements (R. Sladkovic, IFU) at two nearby mountain sites (Zugspitze, 2964 m a.s.l. and Wank, 1780 m a.s.l., both 47° N, 11° E). 195 episodes with intrusions of stratospheric air were identified at the Zugspitze, corresponding

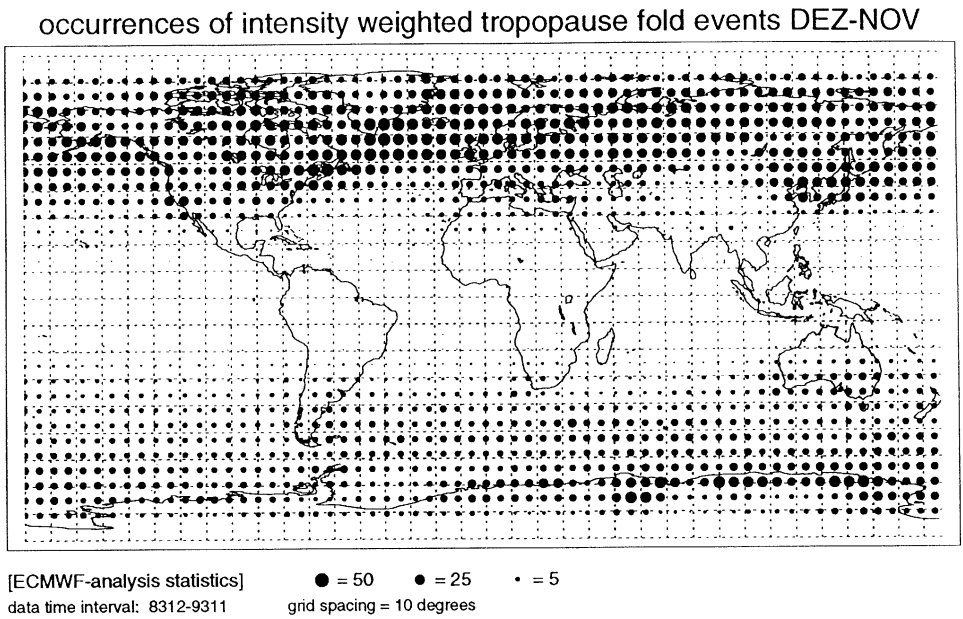

Figure 2. Annual mean distribution of the global tropopause folding activity obtained with the EURAD group algorithm for the years 1984–1993; the size of the dots denotes the activity corresponding to the intensity weighted sum (sum of class numbers) of mean annual events.

to 5% of all considered days. At the Uccle station, folds are detected with similar frequency over the free troposphere with the KMI/CNRS algorithm, which implies that most of the folds reach down into at least below 5 km height. Nevertheless, only 1.4% of the soundings show a fold in the 3–5 km region (with the KMI/CNRS algorithm), much less than the enhanced ozone/^{7}Be episodes observed at 3 km height. As appears from Section 5, probably even less tropopause folds in the lower troposphere would have been observed in southern Germany. This difference documents that stratospheric tracers like ozone and ^{7}Be are diluted in the lower free troposphere over a much larger area as that covered by tropopause folds (restricted to the polar front in the algorithms of KMI/CNRS and University of Cologne). The dilution of the stratospheric air with tropospheric background air during this transport is documented by the fact that the average increase in the ozone concentration is about 10 ppb in the stratospheric intrusions compared to several tenths of ppb in folds. For example, for folds observed with the KMI/CNRS algorithm over Uccle, monthly averages of peak ozone concentrations vary between 120 ppb encountered in May and 78 ppb in December, which is by the way coherent with the lower stratospheric seasonal ozone variation above Uccle. As for folds, the seasonality of this ozone increase in stratospheric intrusions (about 12 ppb in late winter and spring and 8 ppb in fall) still follows roughly the seasonal variation of ozone in the lower stratosphere. The seasonal frequency distribution of the stratospheric intrusions into the lower troposphere shows at the Zugspitze

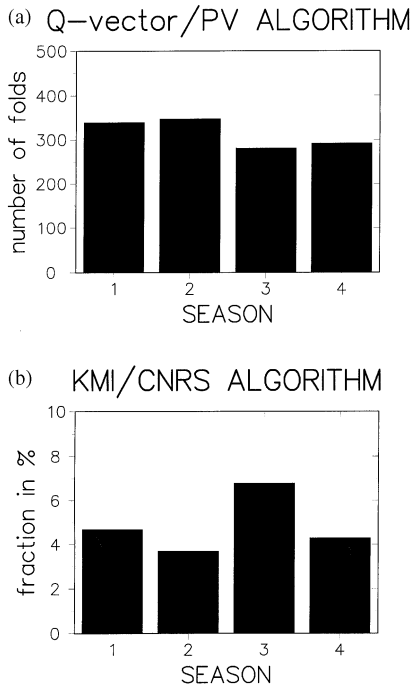

Figure 3. Seasonal occurrence of tropopause folds in Western Europe; number of folds (1984–1991) in the $\pm 10^{\circ}$ rectangle around Uccle from the Q-vector divergence/PV algorithm (a); the fraction of folds among ozone/PTU soundings (1969–1994) taken at Uccle detected by the KMI/CNRS algorithm (b); 1 = winter (Dec., Jan., Feb.), etc.; for the comparability of absolute numbers to fraction of fold among ozone/PTU soundings, see text in Section 4.

a maximum in January and a minimum in late spring/summer (Figure 3) which corresponds rather well to the seasonal variation of folds detected with the Q-vector divergence/PV algorithm (see Section 5). At the Wank summit, less than a half of intrusion episodes (85 cases) than at Zugspitze were observed. The more pronounced late spring/summer minimum at Wank may reflect the larger elevation of the boundary layer capping inversion layer during spring and summer preventing transport to the Wank summit.

4. Comparison of the Tropopause Fold Detection Algorithms

This section is devoted to an intercomparison of the three tropopause fold detection algorithms. First, we will analyse results for the Uccle station and for the years 1989–1992 when both the University of Cologne and the KMI/CNRS algorithm were applied. During this period, among 554 soundings, 22 folds are detected with the KMI/CNRS algorithm and 9 with the University of Cologne algorithm. With one exception (borderline case with respect to the stability condition), all of the 9 folds detected by University of Cologne are also detected by KMI/CNRS,

whereas 14 'KMI/CNRS folds' are not retained by University of Cologne. The major difference in the set-up of both algorithms is that the University of Cologne algorithm requires a potential vorticity maximum in the folding region whereas the KMI/CNRS algorithm requires enhanced stability and a vertical wind shear (see Section 2). It appears thus that the PV criterium is more restrictive than the combined stability/vertical wind shear. PV is computed by the University of Cologne group from standard isobaric ECMWF analysis vertically interpolated onto isentropic levels following a procedure developed by Bleck (1984). One possible reason for the discrepancies in the algorithms is then that the ECMWF input data with about 1.5 to 2 km vertical resolution in the middle troposphere and tropopause region may not well resolve tropopause folds with a vertical resolution of down to several hundred meters. Folds detected with the University of Cologne algorithm should then be on the average more pronounced than folds detected with the KMI/CNRS algorithm. Some of the differences may also be due to the fact that both (automatic) algorithms are designed to detect the average number of tropopause folds, but that they will certainly miss or wrongly detect a fraction of borderline cases. Thus, discrepancies in the results cannot be attributed unambiguously to one or the other algorithm. Consequently, fold statistics from both algorithms will be treated in the remainder of this paper as independent data sets.

Folds detected with the University of Cologne or KMI/CNRS algorithm are in nearly all cases also detected with the Q-vector divergence/PV algorithm in a 500 km radius around Uccle and OHP. On the contrary, folds detected by the Q-vector divergence/PV algorithm in that radius around these stations are often not observed with the University of Cologne or KMI/CNRS algorithm. However, this fact is *not* to be taken as a discrepancy between the algorithms as there is a 12 h gap between soundings ($\sim$12 UT) and analyses used for the Q-vector divergence/PV algorithm (00 UT). Sounding stations may then often not measure at the right place with respect to folds. To put this comparison on a more quantitative basis, the number of folds present on the average in a certain horizontal domain around a sounding station has to be considered. This number (n) is directly obtained from the Q-vector divergence/PV statistics and will be derived from the statistics based on the KMI/CNRS algorithm (for which the data base is large enough for this type of comparison) by applying the formula:

$$n = f \cdot A/A_d\,, \tag{1}$$

where f is the fraction of ozone profiles showing a fold, A_d is 'detectable area' of a fold and A the surface of the considered region. 'Detectable area' denotes the area with respect to the fold in which a sounding has to take place in order to allow the fold to be detected. Inspection of 300 hPa weather maps shows that folds are detected with the KMI/CNRS algorithm if the ozone/radiosonde was launched in an area extending from 100–150 km both on the cyclonic and anticyclonic side of the jet stream axis. Successive vertical cross-sections (PV, potential temperature, wind) show that folds typically extend 1000–1500 km along the jet axis. This

corresponds to a detectable area of folds A_d equal to $3.1 \pm 0.9 \times 10^5$ km^2 (250 ± 50 km $\times$ 1250 ± 250 km) for the KMI/CNRS algorithm. The uncertainty in A_d was obtained from the quadratic sum of the relative uncertainties (about 20%) in the fold extension across and along the jet axis.

The folding fractions f at Uccle and at OHP for soundings from 1984–1994 are 0.056 ± 0.007 and 0.03 ± 0.01, respectively. Under the assumption that the number of folds obeys Poisson statistics, the relative uncertainties are given as $1/\sqrt{N}$ with $N = 60$ for Uccle and $N = 10$ for the OHP for the 1984–1994 period. Applying formula (1) yields then an average number of 0.50 ± 0.16 folds simultaneously present in a $\pm 10^\circ$ rectangle around Uccle ($A = 2.8 \times 10^6$ km^2) and 0.30 ± 0.13 in a corresponding rectangle around the OHP ($A = 3.1 \times 10^6$ km^2). Again, uncertainties in these estimations were obtained by taking the quadratic sum of the relative uncertainties in A_d and f. For the Q-vector divergence/PV algorithm, a roughly 10% uncertainty in the number of detected folds is assumed by considering that the overlap between detected folds and the reference base of folds generated from EURAD model simulations is not complete (Ebel *et al.*, 1996). The corresponding numbers are thus 0.43 ± 0.04 for Uccle and 0.32 ± 0.03 for the OHP. Taking into account the uncertainty in the detectable area of the folds derived above and additionally the large statistical uncertainty in the folding frequency for the OHP, these results do not indicate any systematic bias between both algorithms. This semi-quantitative consistency in the results is comforting as both algorithms are based on different principles (the Q-vector divergence/PV algorithm being process (frontogenesis) oriented and the KMI/CNRS algorithm tracer (ozone) oriented).

5. Regional Scale Changes in the Tropopause Fold Occurrences and Seasonal Variation

Both the Q-vector divergence/PV and the KMI/CNRS algorithm showed (see last section) a larger folding frequency around the more northerly station Uccle (51° N, 4° E) than around OHP (44° N, 6° E) and Biscarosse (43° N, 1° W). A north–south gradient of folding occurrence is also more generally observed in the Q-vector divergence/PV climatology over Europe (Figure 2). On a smaller spatial scale, over Western and Central Europe, results from the University of Cologne algorithm (Table I) also show a tendency for more folds occurring at the more northerly stations Uccle (51° N, 4° E) and Jülich (51° N, 6° E) than at the more southerly stations Hohenpeissenberg (48° N, 11° E) and Payerne (47° N, 7° E) (Speth *et al.*, 1996). However, due to the low (or even zero) absolute number of folds detected for certain stations, spatial differences obtained from ozone/PTU soundings need further confirmation with larger data sets. Nevertheless, already these preliminary results show the interest in addressing regional scale spatial differences in the folding occurrence from combined data sets based on meteorological analyses and ozone/PTU soundings.

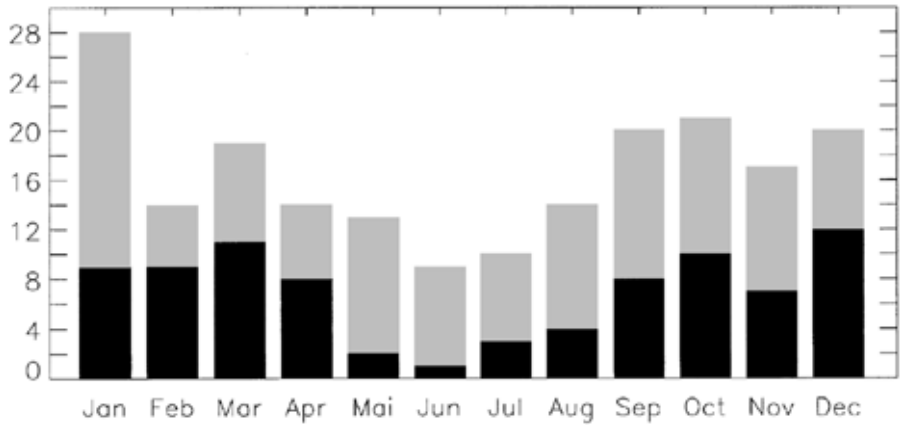

Figure 4. Seasonal variation of number of events of stratospheric air injections at the Zugspitze (2964 m a.s.l., sum of black and grey bars) and at the Wank (1780 m a.s.l., black bars) in the period from 1984 to 1993 obtained from ozone/^{7}Be time series.

The seasonal variation of fold occurrence and activity as derived from the Q-vector divergence/PV algorithm, shows a late-spring-to-summer minimum in the northern hemisphere (Ebel *et al.*, 1996). In Western Europe, in a region of $\pm 10^{\circ}$ around Uccle (51° N, 4° E), this minimum is shifted towards summer/autumn (Figure 4), with a rather small amplitude (20%) of the seasonal variation. Among folding statistics derived from ozone/PTU soundings, only the 25 year time series at Uccle analysed with the KMI/CNRS algorithm is large enough to study the seasonal variation: folds appear with similar frequency in all seasons except for summer (June–August) when their frequency is enhanced to 6.8% compared to the annual mean of 4.8% (Figure 3b). Thus, if we have shown in the last section that on the annual average, the number of folds present around Uccle is similar between the Q-vector divergence/PV and the KMI/CNRS algorithm, differences between both algorithms subsist nevertheless in the seasonal variation, the KMI/CNRS algorithm showing the relatively more cases in summer. Reasons for this discrepancy are not immediately obvious and we would like to postpone the discussion of this point until the disagreement in the seasonal variation is confirmed (or not) for other stations than Uccle.

6. Ozone Flux Across the Tropopause Due to Tropopause Folds

A quantitative estimation of downward transport across the extratropical tropopause should rely on several independent methods. If results from different approaches agree then within their error bars, a coherent and robust picture of this transport is obtained. In the past, estimations of ozone transfer across the tropopause were based on the use of radioactive tracers (Danielsen and Mohnen, 1977), of the N_2O/NO_y/ozone ratio in the lower stratosphere (Murphy and Fahey, 1994), and

Table II. Literature estimates of the cross-tropopause ozone flux within tropopause folds, in 10^{32} molecules per day. The direct comparability of the flux values is limited due to the different representation of transfer rates in the literature made reference to

Author	Method	Month	Ozone flux
Lamarque and Hess (1994)	Mesoscale model simulations	February	1.8[a]
Spaete *et al.* (1994)	Mesoscale model simulations	February	7.9[b]
Ebel *et al.* (1996)	Mesoscale model simulations	April/May	10.4[a]
Ancellet *et al.* (1991)	Ozone lidar + trajectories	March	10.0
Vaughan *et al.* (1994)	Radio soundings + trajectories	October	4.0[c]
Ancellet *et al.* (1994)	Ozone lidar + trajectories	November	6.5

[a] Adjusted for an ozone/PV ratio of 51 ppb/PVU in February and 66 ppb/PVU in April/May at the 1.6 PVU level (from ozone and PV climatologies at Uccle and OHP (Beekmann *et al.*, 1994)).
[b] Obtained from a net mass flux of 3×10^{14} kg d^{-1} across the 3.0 PVU level combined to the ozone/PV ratio of 42 ppb/PVU in February at this level.
[c] Value obtained by assuming here a time scale of the transfer of 1 day on the basis of trajectory calculations presented in Vaughan *et al.* (1994).

of general circulation model (Gidel and Shapiro, 1980; Mahlmann *et al.*, 1980; Allam and Tuck, 1984). Transfer estimations based on the residual mean meridional circulation in the lowermost stratosphere (Rosenlof and Holton, 1993) are available for mass but not yet for tracers. In this paper, we follow yet an alternative approach to derive the cross-tropopause ozone flux associated to folds by combining the above presented tropopause folding climatologies with ozone transfer estimations for individual folding systems.

The average cross-tropopause ozone flux F_{O_3} related to folds can be obtained from the number of folds n present in a region A and the ozone amount T_{O_3} transferred per unit of time during individual folding episodes.

$$F_{O_3} = n \cdot T_{O_3}/A \tag{2}$$

Table II gives an overview of literature estimates for T_{O_3} derived from experimental studies and mesoscale modelling studies. When no ozone measurements were available (Ebel *et al.*, 1996; Lamarque and Hess, 1994; Spaete *et al.*, 1994; Vaughan *et al.*, 1994) the ozone/PV ratio, deduced from several hundred ozone soundings and PV profiles over Uccle and OHP (Beekmann *et al.*, 1994 for the OHP), was used to obtain a value for the ozone transport. In the tropopause region, this ratio has an average value of about 50 ppb/PVU with a distinct seasonal and height variation (for more details see Table II) which is much lower than Danielsen's (1968) value of 120 ppb/PVU. This value has been derived from only a few ozone profiles recorded during a case study in April 1963. A lower value for the ozone/PV ratio than previously assumed is also confirmed by tropopause fold studies (e.g., Browell *et al.*, 1987).

Estimations of T_{O_3} in Table II show a large scatter reflecting (i) random variability in the fold strength, (ii) seasonal variability in the fold strength and (iii)

uncertainties in the methods to derive the ozone transfer in a fold. For example, Ebel *et al.* (1996) partly ascribed the low ozone transfer values given by Lamarque and Hess (1994) to a weaker activity of the folding system investigated in that study than the activity in the two other modelling studies referenced in Table II (Spaete *et al.*, 1994; Ebel *et al.*, 1996). Seasonal variability of the fold strength should not too much influence the average value of T_{O_3} as estimations from different seasons are taken into account with nevertheless more cases in the February–May period. Uncertainty in the estimations based on ozone measurements (Ancellet *et al.*, 1991, 1994) mainly stems from uncertainty in the characteristic time scale (about two days and one day, respectively) of the downward transport across the troposphere in the polar front. This time scale can be deduced from 3D trajectories obtained from analysed wind fields (ECMWF) and the same technique is also applied here for Vaughan *et al.*'s (1994) study yielding a time scale of one day. Estimations with the mesoscale models MM4 and MM5 (Lamarque and Hess, 1994; Ebel *et al.*, 1996) and MASS (Spaete *et al.*, 1994) rely on the capacity of these models to adequately represent transport processes within tropopause folds (i.e., transport across fixed PV-surfaces due to diabatic and turbulent processes). However, a quantification of uncertainties from both experimental or modelling approaches is not yet possible, it requires to carry out dedicated model validation campaigns as for example planned in the ongoing CEE/TOASTE C project (Gray, 1995). Nevertheless, by assuming a normal distribution of methodological errors and of the fold strengths, it is possible to get an estimation of the ozone transfer by averaging over the different values given in Table II, the uncertainty of this estimation being given as the standard deviation of the mean. By doing so, an amount of 6.8×10^{32} molecules ozone transferred per fold and per day into the troposphere with an 1σ uncertianty of 1.4×10^{32} (21%) is obtained.

Applying formula (2), the term T_{O_3} is then combined with the number n of folds occurring in the Northern Hemisphere (18.4 obtained from the Q-vector divergence/PV statistics) yielding an average ozone flux across the tropopause F_{O_3} of 5.7×10^{10} mol. cm^{-2} s^{-1}. The uncertainty (1σ) of this estimation of 1.3×10^{10} mol. cm^{-2} s^{-1} or 23% has been obtained by the quadratic sum of relative uncertainties in T_{O_3} (21%) and n (10%). Obviously, the uncertainty in the ozone amount transferred by fold makes by far the larger contribution. A flux value representative for Western Europe is obtained from the number of folds present in the $\pm 10^\circ$ rectangle around Uccle from the Q-vector divergence/PV study ($n = 0.43$; which is similar to the value from KMI/CNRS statistics, $n = 0.50$) and amounts to $12 \pm 2.7 \times 10^{10}$ mol. cm^{-2} s^{-1}, which is by about a factor of two larger than the Northern Hemispheric flux. It has to be stressed that these flux values only include the ozone exchange due to tropopause folds; other processes, such as erosion of cut-off lows, may give a significant additional contribution.

7. Conclusion and Discussion

The comparison between the process (frontogenesis)-oriented Q-vector divergence/PV algorithm and the tracer (ozone, relative humidity)-oriented algorithm of KMI/CNRS does not reveal any systematic bias in the annual fold occurrence over Western Europe. The University of Cologne algorithm detects less, but probably stronger folds than the KMI/CNRS algorithm, which is related to the use of a potential vorticity criterium in the University of Cologne and a stability/vertical wind shear criterium in the KMI/CNRS algorithm. Injections of stratospheric air into the lower troposphere deduced from ozone/^{7}Be time series at 3 km height appear more often than folds in the same height region which is consistent with the fact that stratospheric tracers spread out from the polar front while being transported to the lower troposphere. For the algorithms based on data sets lasting at least over 10 years (Q-vector divergence/PV, KMI/CNRS at Uccle station), the seasonal variation of the fold occurrence is rather flat, with however differences between both algorithms observed during summer (minimum for Q-vector divergence/PV, maximum for KMI/CNRS algorithm). A pronounced spring maximum which may be expected from the strong spring maximum in STE found by Danielsen and Mohnen (1977) and also by Appenzeller *et al.* (1996) (from the mass flux across the 380 K level and the mass variation of the lowermost stratosphere) does *not* occur, neither in Western Europe, nor on a global scale. Thus, either folds are more effective in transporting ozone across the tropopause during spring or other STE processes than folds are responsible for the spring maximum in STE. The first hypothesis may be tested in future by repeating mesoscale model studies of ozone transfer within folds for different seasons.

The Q-vector divergence/PV algorithm shows the presence of, on the average, 18.4 simultaneous folds in the Northern hemisphere. Combining this value with ozone transfer estimates for single folds given in the literature, an estimate for the cross-tropopause ozone flux of 5.7×10^{10} mol. cm^{-2} s^{-1} over the Northern Hemisphere is obtained, which does not yet include the potential contribution from other STE processes than folds. The uncertainty of this estimate is 1.3×10^{10} mol. cm^{-2} s^{-1} (1σ) and is mainly due to the uncertainty in the cross-tropopause ozone transfer in single fold episodes. The corresponding flux over Western Europe amounts to $12 \pm 2.7 \times 10^{10}$ mol. cm^{-2} s^{-1}.

These estimations based on the analysis of synoptic scale events at the tropopause level will now be compared to estimations from other independent methods. By adjusting Danielsen and Mohnen's (1977) initial estimate of 7.8×10^{10} mol. cm^{-2} s^{-1}, derived from the ^{90}Sr deposition at ground and the ozone/PV/^{90}Sr ratio in the lowermost stratosphere, to a lower ozone/PV ratio (58 ppb/PVU instead of 120 ppb/PVU) a flux of 3.8×10^{10} mol. cm^{-2} s^{-1} is obtained. From 2D chemical modelling of the stratospheric NO production from N_2O and the measured ozone/NO_y ratio, a range of values of 1.9–6.4 $\times 10^{10}$ mol. cm^{-2} s^{-1} on a global scale was derived (Murphy and Fahey, 1994) which may be possibly larger for the

Northern Hemisphere alone. Three general circulation model (GCM) simulations gave a cross-tropopause ozone flux of respectively 3.8 (Allam and Tuck, 1984), 4.9 (Gidel and Shapiro, 1980) and 6.6×10^{10} mol. cm^{-2} s^{-1} (Mahlmann *et al.*, 1980). These estimations obtained with independent approaches show indeed a rather good agreement within their still large error bars (or dispersion of results for estimations based on general circulation models). However, if there were other significant contributions to strat-trop exchange than from tropopause folds then our flux estimation could become larger than the other estimations.

Based on the picture of relatively coherent ozone transfer estimates it will be tempting for future work to investigate the competition between photochemistry and in determining the ozone budget and variability in the free troposphere. This is not a simple task, as tropopause folds are accompanied by rapid downward transport into the lower free troposphere – as for example illustrated by the ozone and ^{7}Be time series obtained at the mountain stations Zugspitze and Wank – which has to be accounted for in model calculations assessing the fate of stratospheric ozone transferred into the troposphere.

Acknowledgement

The European Centre for Medium-Range Weather Forecast (ECMWF) is acknowledged for meteorological analysis data. The Observatory of Hohenpeissenberg of the German Weather Service and the Aerological Station Payerne of the Swiss Meteorological Institute are thanked for support with ozone/ratio-sounding data.

References

Allam, R. J. and Tuck, A. F., 1984: Transport of water vapour in a stratosphere-troposphere general circulation model, I. Fluxes, *Q. R. J. Meteorol. Soc.* **110**, 321–356.

Ancellet, G., Pelon, J., Beekmann, M., Papagiannis, A., and Mégie, G., 1991: Ground based lidar studies of ozone exchanges between the stratosphere and the troposphere, *J. Geophys. Res.* **96**, 22401–22421.

Ancellet, G., Beekmann, M., and Papagiannis, A., 1994: Impact of a cutoff low development on downward transport of ozone in the troposphere, *J. Geophys. Res.* **99**, 3451–3468.

Appenzeller, C., Holton, J. R., and Rosenlof, K., 1996: Seasonal variation of mass transport across the tropopause, *J. Geophys. Res.* **101**, 15701–15708.

Beekmann, M., Ancellet, G., and Mégie, G., 1994: Climatology of ozone in Southern Europe and its relation to potential vorticity, *J. Geophys. Res.* **99**, 12841–12853.

Beekmann, M., Ancellet, G., Blonsky, S., De Muer, D., Ebel, A., Elbern, H., Hendricks, J., Kowol, J., Mancier, C., Sladkovic, R., Smit, H. G. J., Speth, P., Trickl, T., and Van Haver, P., 1997: TOR Task group 3b: Stratosphere-troposphere exchange – regional and global tropopause folding occurrence, EUROTRAC final report, part 9, TOR project, to be published.

Bleck, R., 1994: Vertical coordinate transformation of vertically-discretisized atmospheric fields, *Mon. Wea. Rev.* **112**, 2535–2539.

Speth, P., Blonsky, S., and Kunz, H., 1996: Bestimmung des anthropogenen und natürlichen Anteils am Ozon im Mitteleuropäischen Raum aus meteorologischer Sicht. Abschlussbericht und wissenschaftliche Ergebnisse, 1994–1996, BMFT Forschungsvorhaben 07EU777A0.

Browell, E., Danielsen, E., Ismail, S., Gregory, G., and Beck, R., 1987: Tropopause fold structure derived from airborne Lidar and *in situ* measurements, *J. Geophys. Res.* **92**, 2112–2120.

Danielsen, E., 1968: Stratosphere-troposphere exchange based on radioactivity, ozone and potential vorticity, *J. Atmos. Sci.* **25**, 502–518.
Danielsen, E. and Mohnen, V., 1977, Project Dustorm Report: Ozone transport, *in situ* measurements, and meteorological analysis of tropopause folding, *J. Geophys. Res.* **82**, 5867–5877.
Ebel, A., Elbern, H., and Oberreuther, A., 1993: Stratosphere-troposphere air mass exchange and cross-tropopause flux of ozone, in E. V. Thrane, T. A. Blix, and D. C. Fritts (eds), *Coupling processes in the Lower and Middle Atmosphere*, Kluwer Acad. Publ., Dordrecht, pp. 49–65.
Ebel, A., Elbern, H., Hendricks, J., and Meyer, R., 1996: Stratosphere-troposphere exchange and its impact on the structure of the lower stratosphere, *J. Geomag. Geoelectr.* **48**, 135–144.
Elbern, H., Kowol, J., and Ebel, A., 1996: Deep stratospheric intrusions: A statistical assessment with model guided analysis, *Atmos. Environ.*, in press.
Gidel, L. and Shapiro, M., 1980: General circulation estimate of the net vertical flux in the lower stratosphere and implications for the tropospheric ozone budget, *J. Geophys. Res.* **85**, 4049–4058.
Gray, L., 1995: TOASTE-C, Transport of Ozone and Stratosphere Troposphere Exchange, Proposal to the European Commission for financial support in respect of Community activities in the field of Research into the Environment and Climate: Area 1.2.1. Atmospheric Physics and Chemistry.
Holton, J. R., Douglass, A. R., Haynes, P. H., McIntyre, M. E., Rood, R. B., Pfister, L., 1996: Stratosphere-troposphere exchange, *Rev. Geophys.* **33**, 403–439.
Lamarque, J. F. and Hess, P. G., 1994: Cross-tropopause mass exchange flux and potential vorticity budget in a simulated tropopause folding, *J. Atmos. Sci.* **51**, 2246–2269.
Mahlman, J. D., Levy, H. B., and Moxim, W. J., 1980: Three-dimensional tracer structure and behaviour as simulated in two ozone precursor experiments, *J. Atmos. Sci.* **37**, 655.
Murphy, D. M. and Fahey, D. W., 1994: An estimate of the flux of stratospheric reactive nitrogen and ozone into the troposphere, *J. Geophys. Res.* **99**, 5325–5332.
Price, J. D. and Vaughan, G., 1992: Statistical studies of cut-off low systems, *Ann. Geophys.* **10**, 96–102.
Rosenlof, K. H. and Holton, J. R., 1993: Estimates of the stratospheric residual circulation using the downward control principle, *J. Geophys. Res.* **98**, 10465–10479.
Shapiro, M. A., 1980: Turbulent mixing within tropopause folds as a mechanism for the exchange of chemical constituents between the stratosphere and the troposphere, *J. Atmos. Sci.* **37**, 994–1004.
Shapiro, M. A., Hampel, T., and Krueger, A. J., 1986: The Arctic tropopause fold, *Mon. Wea. Rev.* **115**, 444–454.
Spaete, P., Johnson, D. R., and Schaack, T. K., 1994: Stratospheric-Tropospheric Exchange during the President's day storm, *Mon. Wea. Rev.* **122**, 424–439.
Van Haver, P., Beekmann, M., De Muer, D., and Mancier, C., 1996: Climatology of tropopause folds at midlatitudes, *Geophys. Res. Lett.* **23**, 1036–1036.
Vaughan, G., Price, J. D., and Howells, A., 1994: Transport into the troposphere in a tropopause fold, *Q. R. J. Meteorological Soc.* **120**, 1085–1103.
Viezee, W., Johnson, W. B., and Singh, H. B., 1983: Stratospheric ozone in the lower troposphere II, Assessment of downward flux and ground level impact, *Atmos. Environ.* **17**, 1979–1993.